

Formation of vacancy-impurity complexes in heavily Zn-doped InP

J. Slotte, K. Saarinen, A. Salmi, S. Simula, R. Aavikko, and P. Hautojärvi

Laboratory of Physics, Helsinki University of Technology, P.O. Box 1100, FIN-02015 HUT, Finland

(Received 19 June 2002; revised manuscript received 20 December 2002; published 26 March 2003)

Positron annihilation spectroscopy has been applied to observe the spontaneous formation of vacancy-type defects by annealing of heavily Zn-doped InP at 500–700 K. The defect is identified as the V_P -Zn pair by detecting the annihilation of positrons with core electrons. We conclude that the defect is formed through a diffusion process; a phosphorus vacancy migrates until trapped by a Zn impurity and forms a negatively charged V_P -Zn pair. The kinetics of the diffusion process is investigated by measuring the average positron lifetime as a function of annealing time and by fitting a diffusion model to the experimental results. We deduce a migration energy of 1.8 ± 0.2 eV for the phosphorus vacancy. Our results explain both the presence of native V_P -Zn pairs in Zn-doped InP and their disappearance in post-growth annealings.

DOI: 10.1103/PhysRevB.67.115209

PACS number(s): 61.72.Ji, 66.30.Lw, 71.55.Eq, 78.70.Bj

I. INTRODUCTION

The redistribution of impurities and defects through diffusion processes plays an important role in the material properties of semiconductor devices. Diffusion can both be a tool in device fabrication, e.g., incorporation of dopants through diffusion, or it can harm the electrical properties of the device by, e.g., the broadening of sharp impurity distributions. In order to be able to control the diffusion processes in a semiconductor thorough knowledge of the diffusion energetics is of vital importance.

Point defects, such as vacancies, influence the electrical properties of semiconductors. In semiconductors the formation energy of charged defects and thus the concentration of defects depend on the Fermi level. At high doping concentrations, when the Fermi level is close to conduction or valence bands, compensating centers may be abundantly created. These defects decrease the fraction of dopants able to deliver free carriers to conduction and valence bands. The formation energies of defects are thus essential for understanding the electrical properties of heavily doped semiconductors. Theoretical calculations can predict this quantity as a function of the Fermi level position,¹ but the direct experimental determination of defect formation energies is generally difficult. Equally difficult is the direct observation of vacancy diffusion. Diffusion parameters for vacancies are often indirectly determined from impurity diffusion studies.² Since vacancies generally are mobile at much lower temperatures than impurities, vacancy diffusion can influence the electrical properties over a wider temperature range. Examples of such a process is the pairing of a vacancy and dopant through a migration process.

Zn-doped InP is a well-known example of a semiconductor, where electrical compensation of Zn acceptors is significant at high doping concentrations in the mid- 10^{18} - cm^{-3} range. Previous experiments have revealed vacancies complexed with Zn impurities after the growth of such a material.^{3–5} However, the formation energies and mechanisms of the complexes are not known. Further, their disappearance in the post-growth annealing at 700 K is surprising^{3,5} since the material is originally fabricated at much higher temperature.

The creation and kinetic behavior of P vacancies on clean InP surfaces have also been the focus of a few studies.^{6–9} Some of these studies show that the P vacancy is mobile already at fairly low temperatures, 400–550 K, and that this can result in defect complexes involving the Zn dopant.^{7,10}

Positron annihilation spectroscopy (PAS) enables the direct identification and quantification of vacancy defects.^{11,12} Thermalized positrons get trapped at vacancies where the positive charge of the ion cores is missing. At vacancies the electron density is reduced compared with that of the perfect lattice. Hence, the positron lifetime increases and the momentum distribution of the annihilating e^+e^- pair narrows. Positron spectroscopy has been one of the major techniques for obtaining information on the vacancy formation energies in metals.¹³ For the case of silicon a few attempts^{14,15} have been made to determine formation energies of vacancies, but the positron experiments have not been successful. Recently, however Gebauer *et al.* used positron annihilation spectroscopy to study the formation of thermal vacancies in GaAs.^{16,17}

In this work we apply positron spectroscopy to study the formation of P vacancy complexes around 600 K in heavily Zn-doped *p*-type InP. We observe that the P vacancy forms complexes with Zn dopants and determine the activation energy of this process. The complex is identified as a pair consisting of the P vacancy and a Zn dopant. We infer that the vacancy Zn complex is formed when a P vacancy migrates until trapped by a Zn impurity to form a V_P -Zn pair. By applying a diffusion model to the increase in V_P -Zn defect complex concentration, we deduce a migration energy for the phosphorus vacancy of 1.8 eV. Our results provide natural explanations (i) for the presence of V_P -Zn pairs as native defects in Zn-doped InP wafers and (ii) for the disappearance of the native V_P -Zn pairs in post-growth annealings.

II. EXPERIMENTAL DETAILS

Positron experiments were performed in liquid-encapsulated Czochralski-grown InP bulk crystals doped with Zn in the range of 10^{18} cm^{-3} . A summary of the samples is presented in Table I. Since the Zn concentration was crucial for the diffusion modeling, it was determined by

TABLE I. The samples used in the study. The carrier concentrations are given for unannealed samples. $[V_{P-Zn}]_{\text{native}}$ is the native concentration of V_{P-Zn} pairs before annealing and $[V_{P-Zn}]_{\text{max}}$ is the saturated maximum concentration of V_{P-Zn} pairs after a long annealing.

p (10^{18} cm^{-3})	$[Zn]$ (10^{18} cm^{-3})	$[V_{P-Zn}]_{\text{native}}$ (10^{15} cm^{-2})	$[V_{P-Zn}]_{\text{max}}$ (10^{17} cm^{-3})
1.2	-	<	-
3.6	-	<	-
4.5	6.3	3.4	1.2
5.2	6.8	7.2	1.3
6.5	9.5	29	-

secondary ion mass spectrometry (SIMS). The concentration scale in the SIMS measurements was obtained by using a reference sample fabricated by ion implantation of Zn in InP. From the SIMS measurements and Hall measurement values provided by the manufacturer (Nippon Mining Co. Ltd.) of the InP wafers it was evident that 20%–30% of the Zn was compensated.

Two identical samples were sandwiched with a ^{22}Na positron source. The positron lifetime was measured using a fast-fast coincidence system with a time resolution of 230 ps. The positron-electron momentum distribution was measured by recording the Doppler broadening of the 511 keV annihilation radiation with a Ge detector, which had an energy resolution of 1.5 keV at 500 keV. The line shape parameters S (low momentum, central region of the annihilation line) and W (high momentum, wing regions of the annihilation line) were used to describe the Doppler broadening. The momentum windows for the S and W parameters were chosen to $(0-3.4) \times 10^{-3} m_0 c$ and $(11-27) \times 10^{-3} m_0 c$. A coincidence setup consisting of Ge and NaI detectors was utilized to reduce the background, in order to study the annihilations with core electrons in the momentum range of $(10-35) \times 10^{-3} m_0 c$.

All annealings were done *in situ* in vacuum.

III. DEFECT FORMATION AND IDENTIFICATION

Figure 1 shows the average positron lifetime at 300 K after subsequent 1800 s isochronal annealing steps at 300–660 K. Depending on the doping level the positron lifetime is 2–12 ps higher than the InP bulk lifetime ($\tau_B = 245 \text{ ps}$) already before the annealings. Two lifetime components could be extracted from the spectra of the unannealed samples. The longer component τ_2 , having a value of 330 ps at 300 K, corresponds to positron annihilation at vacancy-type defects. The positron lifetime starts to further increase after annealing above 550 K. This shows that vacancy-type defects exist in the as-received samples and more defects are formed during annealings. As can be seen in Fig. 1, the formation depends on the Zn and carrier concentrations and is more efficient at higher doping levels. No detectable vacancies are generated at Zn concentration below $2 \times 10^{18} \text{ cm}^{-3}$.

The thermally generated vacancies can be identified by combining positron lifetime (Fig. 2) and core electron momentum distribution (Fig. 3) measurements. After annealing for 30 min at 700 K the positron lifetime spectra were recorded as a function of temperature between 80 and 600 K. The lifetime spectra, measured at 200–600 K, could be decomposed into two components (Fig. 2). The longer lifetime τ_2 corresponds to positrons annihilating as trapped at vacancy type defects. Below 300 K, τ_2 has the same value (330 ps) as in the unannealed samples, indicating that the defect in the as received samples is the same as the one created in the annealing.

In the temperature interval 80–300 K, τ_2 is evidently constant and τ_{av} increases. This behavior is typical when positrons get trapped at negative ions in addition to vacancies.¹¹ The negative ions, in this case most likely the Zn_{In}^- acceptors, capture positrons at their shallow hydrogenic states. This trapping reduces the fraction of annihilations at vacancies, thus decreasing the average lifetime at low temperatures. This behavior is also seen in the unannealed samples. In order to check the significance of the Zn acceptor as a shallow positron trap we performed a quantitative analysis of the average positron lifetime data in Fig. 2 which included

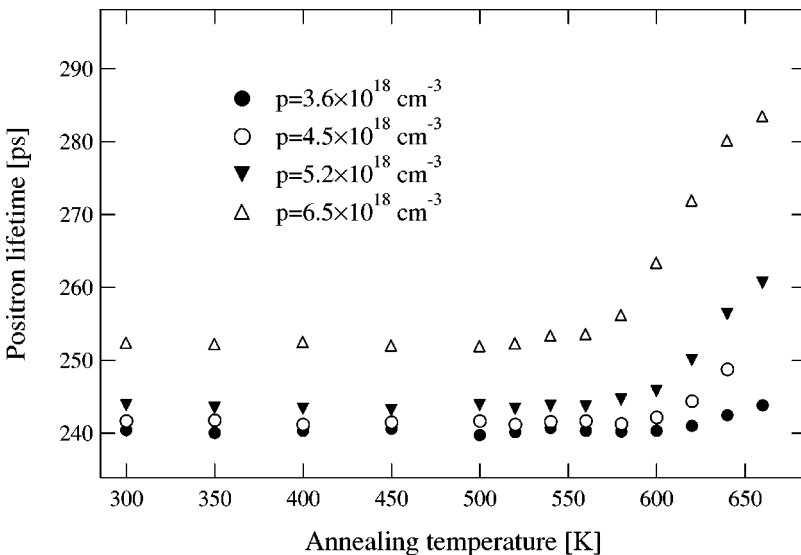


FIG. 1. The average positron lifetimes as a function of the isochronal (1800 s) annealing temperature in various Zn-doped InP samples. The measurement temperature was 300 K.

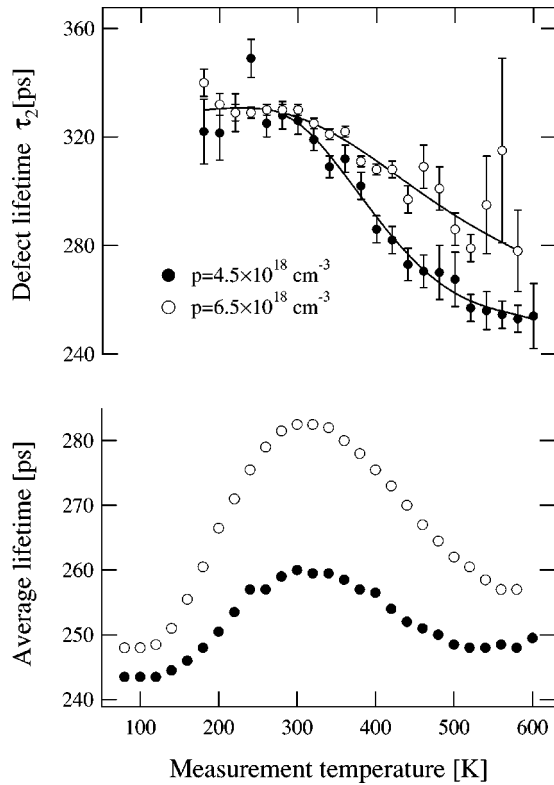


FIG. 2. Average positron lifetime and the lifetime component τ_2 as a function of temperature. The samples were annealed at 700 K prior to lifetime measurements. The solid lines are guides to the eye.

shallow positron traps with binding energies (~ 60 meV) estimated from simple effective mass theory.¹¹ This analysis showed that the trapping to these hydrogenic states at 300 K and at higher temperatures was negligible.

At the measurement temperatures 300–600 K both the average lifetime τ_{av} and the vacancy lifetime τ_2 decrease (Fig. 2). In the decomposition of the lifetime spectra this is seen as a shift in τ_2 from 330 ps to 260 ps. As can be seen from Fig. 2 the shift from 330 to 260 ps occurs at a slightly higher temperature in more heavily doped sample. Similar results have been obtained, e.g., for Si- and Sn-doped *n*-type GaAs.¹⁸ The phenomenon can be explained in the following way: At low temperatures, when the Fermi level is close to the valence band, the vacancy has a configuration corresponding to the lifetime $\tau_2 = 330$ ps. When the Fermi level moves toward the midgap with increasing temperature, the vacancy converts into a more negative charge state, whose atomic configuration corresponds to the lifetime 260 ps. When the Zn doping increases, the Fermi level is closer to the valence band, and the transition 330 ps \leftrightarrow 260 ps shifts toward higher temperatures. The decrease of τ_2 by 70 ps indicates a strong inwards relaxation of the vacancy. A simple estimation of the Fermi level position at 500–600 K indicates that the 0/ $-$ ionization level of the V_P -Zn pair is 0.2 ± 0.1 eV above the valence band.

The core electron momentum distributions were measured at 300 K and 500 K in order to probe both charge states of the thermally generated vacancies (Fig. 3). In bulk InP as well as in the isolated P and In vacancies the positron anni-

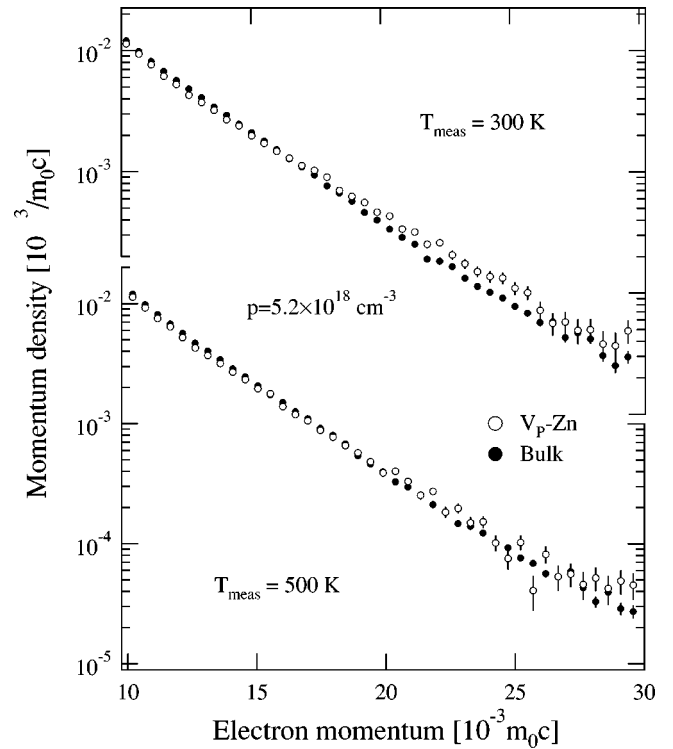


FIG. 3. Core electron momentum distributions probed by positrons in bulk InP and in the V_P -Zn pairs existing in the sample with the carrier concentration $5.2 \times 10^{18} \text{ cm}^{-3}$ and Zn concentration $6.8 \times 10^{18} \text{ cm}^{-3}$, both measured at 300 and 500 K. The Zn-doped sample was annealed at 700 K prior to the experiments. All curves are normalized to the same total area. When not shown, the size of the error-bar is less than the size of the marker.

hilations with In 4d core electrons dominate the momentum distribution at $(10\text{--}30) \times 10^{-3} m_0 c$.⁴ As seen in Fig. 3, the momentum distribution at the vacancies created by annealing at 700 K is broader than observed for bulk InP. The Zn 3d electrons are more localized than In 4d and thus the broadening seen in Fig. 3 is a clear sign of Zn atoms surrounding the vacancy.⁴ Furthermore, the large intensity of the momentum distribution is the fingerprint of the P vacancy, since it is surrounded by In atoms having the relatively high density of In 4d core electrons.¹⁹ The vacancies characterized by the lifetime 330 ps (at 300 K) and 260 ps (at 500 K) are thus two different charge states of the V_P -Zn pair. Since positrons are not trapped by positive vacancies, we assign the charge states as $(V_P\text{-Zn})^0$ (330 ps) and $(V_P\text{-Zn})^-$ (260 ps). As expected the transition from neutral to negative charge state (Fig. 2) occurs at slightly lower temperature for the sample doped to $p = 4.5 \times 10^{18} \text{ cm}^{-3}$, since the Fermi level is initially farther away from the valence band than in the sample doped to $p = 6.5 \times 10^{18} \text{ cm}^{-3}$.

IV. FORMATION KINETICS OF THE V_P -Zn PAIR

A. Isothermal annealing results

In order to study the formation process of the V_P -Zn pair in more detail, we have measured the positron lifetime as a function of annealing time. The samples were annealed at

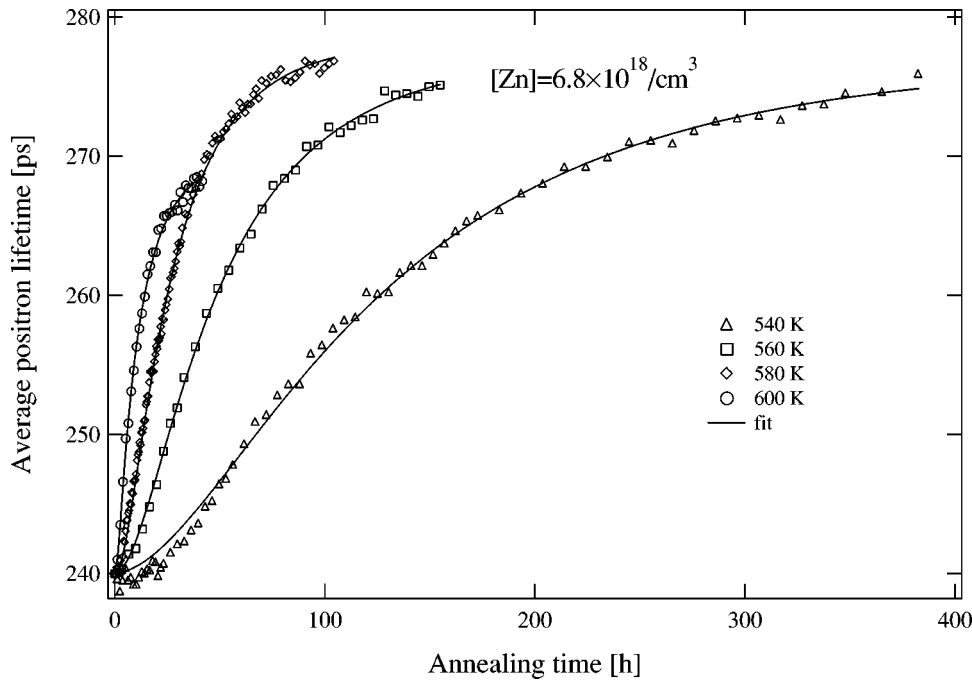


FIG. 4. Average positron lifetime as a function of isochronal annealing time for four different temperatures. In between annealings the samples were measured at 300 K. The solid lines are fits of the diffusion model. The Zn and carrier concentrations in the samples were $6.8 \times 10^{18} \text{ cm}^{-3}$ and $5.2 \times 10^{18} \text{ cm}^{-3}$, respectively.

constant temperature in time intervals ranging from 1 to 20 h. In between annealings the positron lifetime and Doppler broadening parameters were measured at 300 K. The annealing process was continued until the average positron lifetime was saturated. For each Zn concentration the annealing procedure was carried out at four different annealing temperatures.

An example of the average positron lifetime as a function of annealing time for $[Zn] = 6.8 \times 10^{18} \text{ cm}^{-3}$ can be seen in Fig. 4. As can be noted the rate of increase in the average lifetime depends on the annealing temperature. However, an interesting feature of the time development of the average lifetime can be seen if one examines the beginning of the annealing curve in more detail. In Figs. 5(a) and 5(b) we show the first part of the annealing curves of samples with $[Zn] = 6.8 \times 10^{18} \text{ cm}^{-3}$ annealed at 540 and 580 K. As can be seen the average lifetime stays approximately constant in the beginning of the annealing and then starts to increase rapidly. The length of the incubation time also depends on the annealing temperature; the higher the annealing temperature, the shorter is the incubation time. This is an indication that the formation of the V_P -Zn pair consists of two different thermally activated processes. Above 620 K the incubation time has decreased beyond the detection limit of the experiment.

As can be seen from Fig. 4 the saturation lifetime and thus also the concentration of V_P -Zn pairs are independent of the annealing temperature. Furthermore, the saturation concentration of V_P -Zn pairs is in the $\sim 10^{17} \text{ cm}^{-3}$ range (Table I) i.e., less than 10% of the Zn atoms have paired with a P vacancy.

B. Formation of V_P -Zn pairs by the migration of V_P

As noted in Sec. III, the V_P -Zn pair is in a negative charge state when it is formed in the annealings above 550 K (Fig. 1). Since the formation energy of an acceptor-type defect has

its highest value in *p*-type conditions with the Fermi level close to the valence band, we consider it unlikely that the V_P -Zn pair is formed directly in the annealing.

On the other hand, the isolated P vacancy is a positively charged donor and a compensating defect in *p*-type InP, and its formation energy should decrease when the Fermi level approaches the valence band.^{20,21} The concentration of P vacancies should thus increase with Zn doping.^{2,22} This trend is clearly seen in the experiments of Fig. 1 for the V_P -Zn pair.

We thus infer that at higher Zn concentrations there are more P vacancies in the samples. Due to their positive charge state, the isolated P vacancies are not detected by positrons.

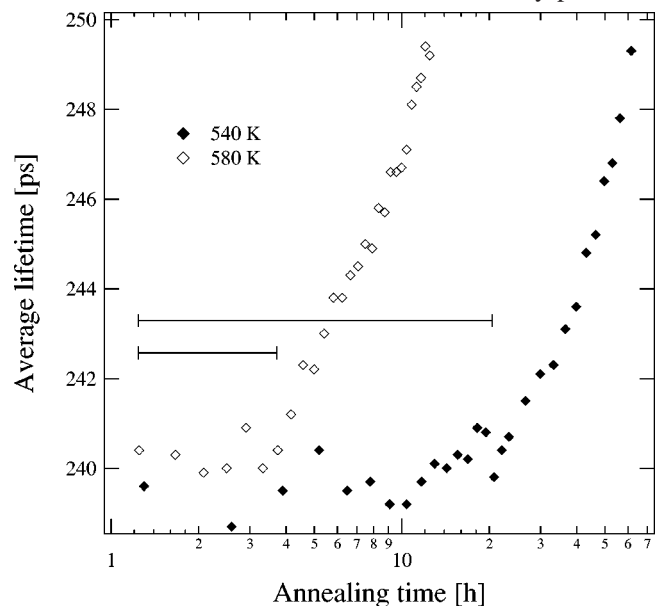


FIG. 5. Average positron lifetime as a function of isochronal annealing time in the beginning of the experiment for 540 and 580 K for the samples in Fig. 4. The bar indicates the approximate incubation time.

During cooling from the crystal growth temperature and during post-growth annealing, migrating P vacancies get trapped at negative Zn impurities, forming neutral or negatively charged V_P -Zn pairs which are observed by positrons. The concentration of thermally generated V_P -Zn pairs will thus depend on the concentration of free P vacancies and on the probability of forming a V_P -Zn pair through the migration of the P vacancy.

Earlier studies have shown that V_P -Zn complexes can be formed when a P vacancy is formed on a clean InP(110) surface and diffuses into the bulk, where it pairs with a Zn dopant.^{7,10} The complexes observed in our study are most likely not formed by P vacancy diffusion from the surface, since the average depth probed by positrons is several tens of micrometers, which would require diffusion lengths for the P vacancy of the order of 100 μm . Furthermore, if the V_P -Zn complex was formed by a P vacancy migrating from the surface one would expect that the saturation concentration of complexes should be approximately equal to the Zn concentration, since the surface in our experiment should be an infinite source of vacancies. As can be seen from Table I, this is not the case. We have nevertheless tried to fit a model with the vacancies diffusing from the surface. However, vacancy diffusion from the surface does not lead to an incubation time, because positrons probe the whole depth of the sample.

The lack of temperature dependence in the saturation concentration is an indication that the P vacancies are not thermally formed in the samples during the annealing process. If this were the case, one would expect more P vacancies and thus more vacancy complexes to be formed in the samples annealed at higher temperatures, which is not observed.

Based on the arguments above we infer that the concentration of the V_P -Zn pairs is limited by the native P vacancies in the as-grown samples. The incubation time visible in Figs. 4 and 5 in the beginning of the annealings indicates that a thermally activated process is needed to make the native P vacancies mobile.

C. Determination of the migration energy

In order to analyze the measured time development of the average positron lifetime during isothermal annealing, we construct a model that takes into account the incubation time in the beginning of the annealing process and explains the increase of the lifetime due to migration of the P vacancy and pairing with the Zn dopant. Our diffusion model thus consist of three separate stages: (i) the V_P becomes mobile, (ii) it migrates freely in the phosphorus sublattice, and (iii) it is trapped by a Zn dopant.

As a first approximation we assume that the rate of decrease of nonmobile P vacancies is proportional to their concentration, $C_{V_P^{nm}}$; i.e., we have a first-order rate equation

$$\frac{dC_{V_P^{nm}}}{dt} = -\lambda C_{V_P^{nm}}, \quad (1)$$

where λ is the the rate constant of the reaction. It corresponds, e.g., to the release of the V_P from a trap or any other first-order chemical reaction. Notice that we can include this

process in the analysis in this way although its physical details are not identified. We also emphasize that this does not influence the estimate for the migration energy of the V_P .

The generation rate of mobile P vacancies per unit volume in a time interval dt is thus

$$\frac{dC_{V_P^f}}{dt} = -\frac{dC_{V_P^{nm}}}{dt} = C_{V_P^{nm}}(0)\lambda e^{-\lambda t}, \quad (2)$$

where $C_{V_P^{nm}}(0)$ is the concentration of nonmobile P vacancies in the beginning of the annealing experiment ($t=0$). The concentration of P vacancies which have paired with a Zn dopant is now given by

$$C_{V_{P\text{-Zn}}}(t) = \int_0^t \left[\frac{dC_{V_P^f}}{dt'} \right]_{t'=\tau} [1-p(t-\tau)] dt', \quad (3)$$

where $p(t)$ is the time-dependent probability that the P vacancy remains isolated (the survival probability) and t is the annealing time.

For the probability function $p(t)$ we use a simple random walk model where the P vacancy migrates in the P sublattice and pairs with a Zn dopant in the In sublattice. The probability as a function of the number of migration jumps is obtained by a Monte Carlo simulation of the migration process. In the simulation the Zn dopant is treated as stationary and located in the In sublattice. For the simulation, only the P sublattice (fcc) is created and the migrating P vacancy is trapped by Zn when it reaches any of the the four fcc sites neighboring the Zn atom. The lattice used in the simulations consisted of $100 \times 100 \times 100$ unit cells with periodic boundary conditions, corresponding to 4×10^6 P lattice sites, and for each simulated Zn concentration 10^5 runs were made. Examples of simulated survival probabilities are shown in Fig. 6. The survival probability is the probability that the vacancy has not paired after a certain amount of diffusion jumps.

We choose to parametrize the probability function with an exponential

$$p(t) = A e^{-aft}, \quad (4)$$

which very accurately describes the probability function. The parametrization is done in order to make it possible to solve the integral in Eq. (3) analytically and thus speed up the fitting procedure. f in the equation above is the jump frequency of the migrating vacancy and the product ft is thus the number of migration jumps. The exponential behavior of the survival probability is also expected from theory and previous Monte Carlo simulations.^{23,24} The jump frequency has the usual Arrhenius temperature dependence

$$f = f_0 e^{-E_m/k_B T}, \quad (5)$$

where E_m is the migration energy, f_0 the preexponential factor, and k_B the Boltzmann constant. The parameters A , B , a , and b for different Zn concentrations are given in Table II.

The possible diffusion of the Zn atom need not be taken into account in the migration model, since Zn diffuses interstitially in InP (Ref. 25) and the energy of dissociation of

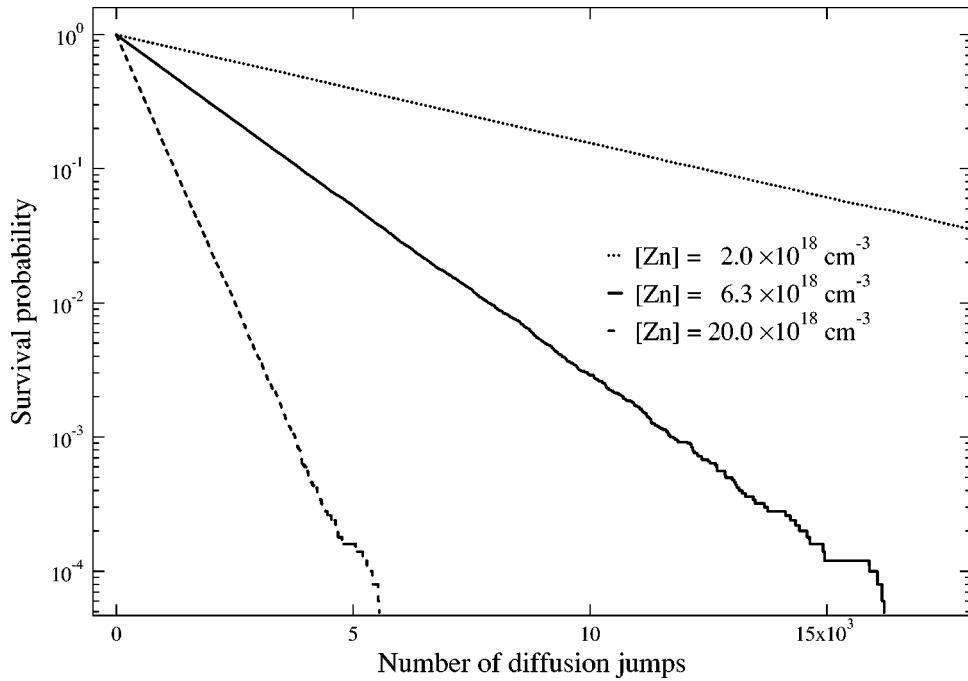


FIG. 6. The simulated probability that the migrating P vacancy remains isolated and not trapped by Zn. The results of the Monte Carlo simulation are shown for various Zn concentrations.

substitutional Zn is assumed too large to make Zn diffusion possible in the temperature interval considered in this experiment.²⁶

The relation between the concentration of V_P -Zn pairs and the average positron lifetime τ_{av} is given by the equation¹¹

$$C_{V_P-Zn} = \frac{\tau_{av} - \tau_b}{\mu \tau_b (\tau_d - \tau_{av})}, \quad (6)$$

where $\tau_b = 245$ ps is the positron lifetime in the InP lattice, $\tau_d = 330$ ps is the lifetime at the V_P -Zn, and $\mu = 2.5 \times 10^{-8}$ cm³/s is the positron trapping coefficient.¹¹ Equations (3) and (4) were inserted into Eq. (6) and the resulting equation was fitted to the experimentally determined average lifetimes. The fitted parameters were the jump frequency f and the rate constant λ .

The fits of the combination of Eqs. (3) and (5) are in good agreement with the data, as seen from the solid lines of Fig. 4. For the fitted jump frequency f we get a good Arrhenius behavior, which is shown in Fig. 7 (solid line). The Arrhenius plot yields a migration energy for the P vacancy of 1.9 ± 0.4 eV and a preexponential of 3.7×10^{15} s⁻¹. The value for the preexponential is somewhat higher than the expected Debye frequency of the crystal; however, we must emphasize that the error in our value is several orders of magnitude. This is due to two reasons: first, the logarithmic nature of the Arrhenius behavior and, second, to that fact that the migra-

tion process can only be studied in a very narrow temperature interval of approximately 100 K.

We have also done simultaneous fits to all data where we have restricted the pre-exponential to the known Debye frequency ($\approx 10^{13}$ Hz) in InP.²⁷ This fit yields a slightly lower activation energy for the migration, 1.8 ± 0.2 eV, which is within the error bars of the unrestricted analysis.

The determination of the activation energy for the λ parameter, which describes the incubation time, is difficult

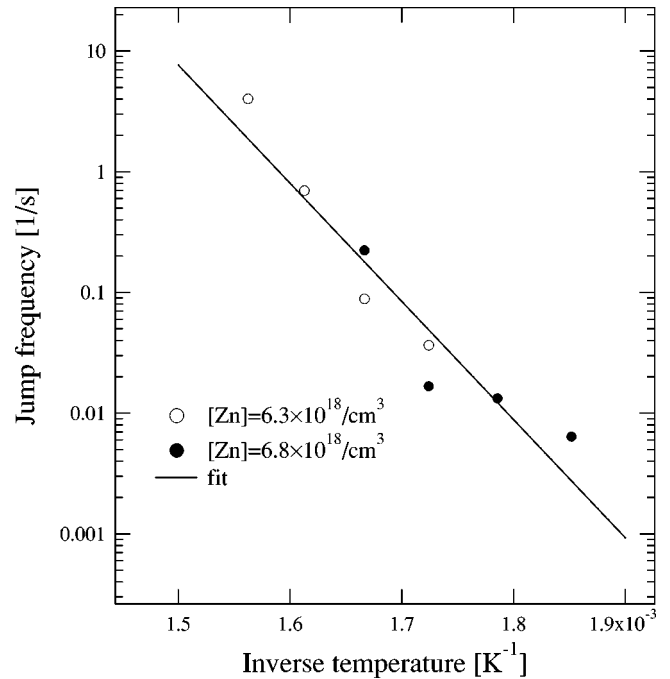


FIG. 7. Arrhenius plot of the jump frequency for samples with Zn concentrations of 6.3×10^{18} cm⁻³ and 6.8×10^{18} cm⁻³. The Arrhenius fit has been made to both sample series simultaneously.

TABLE II. The results of the Monte Carlo parametrization [Eq. (4)] for the samples used in the fitting procedure.

p (10^{18} cm ⁻³)	MC parameters	
	A	$a \times 10^4$
4.5	0.99101	5.8618
5.2	0.97145	6.2563

from the present data, since the incubation time for temperatures above 600 K is so short that the absolute values obtained from the fittings could be ambiguous. An Arrhenius fit to the λ parameter values for anneals below 600 K yield an activation energy of 1.1 eV. The fitted preexponential is 10^5 s^{-1} , which is much lower than the Debye frequency. An activation energy value for the λ parameter can also be obtained by measuring the annealing time required for the average lifetime to increase by 10% directly from the data and by fixing the preexponential to 10^{13} s^{-1} . This yields a value of 1.8 eV. It must, however, be emphasized that these values can only be taken as rough estimates and we estimate that the error in these values for the activation energy of the incubation process is approximately 0.5 eV.

V. $V_{\text{P}}\text{-Zn}$ PAIRS AS NATIVE DEFECTS IN InP

In heavily Zn-doped InP native vacancies are formed during the crystal growth. The formation energy for the P vacancy has its lowest value in *p*-type conditions.²⁸ They can therefore be abundantly created during growth at high temperatures and act as compensating centers. Some of these vacancies can get trapped at Zn atoms or other native impurities as the crystal cools down.

Similarly as in earlier works,³⁻⁵ these defects are observed also in our samples, as shown by the increased values of average positron lifetime already before any annealing treatments (Fig. 1). By combining positron lifetime and Doppler broadening experiments (Figs. 2 and 3) we can show that the native vacancies are $V_{\text{P}}\text{-Zn}$ pairs.⁴ The vacancy complexes formed in the annealing at 540–640 K are thus present already in the as-grown material, but at lower concentration. According to Eq. (6) the concentration of these defects is in the $10^{16}\text{--}10^{17} \text{ cm}^{-3}$ range (Table I) before and after annealing. As seen earlier^{3,5} and confirmed in the present work, the native $V_{\text{P}}\text{-Zn}$ pairs disappear in the heat treatments at 700–800 K.

The present results can be used to explain both the formation and the annealing behavior of native vacancies in heavily Zn-doped InP. Since $V_{\text{P}}\text{-Zn}$ pairs are formed thermally at 540–640 K, it is natural to explain their disappearance at 700–800 K as a result of the dissociation of the pair. At the growth temperature of Zn-doped InP ($T > 1000 \text{ K}$), the concentration of P vacancies is high (probably $> 10^{19} \text{ cm}^{-3}$), but the diffusivity is also very high. Stable $V_{\text{P}}\text{-Zn}$ pairs cannot be formed in these conditions, since the binding energy is too low (breakup temperature 700–800 K). The formation of stable $V_{\text{P}}\text{-Zn}$ pairs can take place only in the relatively narrow temperature interval 500–700 K during the cooling of the crystals. Depending on the cooling rate and Zn dopant concentration, this results in residual $V_{\text{P}}\text{-Zn}$ concentrations in the 10^{16} cm^{-3} range (Table I). The longer the crystal temperature stays in the interval 500–700 K, the more $V_{\text{P}}\text{-Zn}$ pairs will be able to form.

The formation of $V_{\text{P}}\text{-Zn}$ pairs at 550–650 K (Fig. 1) was not observed in the earlier annealing study of Dlubek *et al.*³ Their samples, however, showed a much higher concentration of native $V_{\text{P}}\text{-Zn}$ pairs before any annealings. In fact, these concentrations are close to the maximum values found

in our samples after annealing at 650 K. The larger concentration of native $V_{\text{P}}\text{-Zn}$ pairs in their samples is thus probably due to a slower initial cooling rate of the samples after the growth. Furthermore, the formation of $V_{\text{P}}\text{-Zn}$ pairs (Fig. 1) was also missed by Mahony and Mascher,⁵ who used rapid thermal annealings (RTA's). Most likely the 10 s annealing time was not long enough for the P vacancy to migrate next to a Zn atom.

Dlubek *et al.* observed only partial disappearance of the native $V_{\text{P}}\text{-Zn}$ pairs, when their samples were furnace annealed above 700 K. On the other hand, the work of Mahony and Mascher⁵ shows that all the native $V_{\text{P}}\text{-Zn}$ pairs can be removed by RTA's. We can explain this simply by the dissociation of the $V_{\text{P}}\text{-Zn}$ pairs above 700 K. If the cooling rate from 700 K down to 550 K is fast enough, as evidently in the case of RTA's but not in the furnace annealing, the reformation of the $V\text{-Zn}$ pairs does not occur. The observed formation and dissociation processes of $V_{\text{P}}\text{-Zn}$ pairs demonstrate thus how the post-growth treatment with rapid thermal annealing can improve the defect properties of the material. More macroscopically, this is seen in the electrical experiments⁵ as an increase in the carrier concentration and decrease of compensation.

Previous deep-level transient spectroscopy (DLTS) studies on electron irradiated Zn-doped InP have shown defect levels in the P sublattice. The hole trap $H4$ (0.37 eV above the valence band) has been attributed to the $V_{\text{P}}\text{-Zn}$ pair, and due to the high introduction rate for the defect ($\sim 1 \text{ cm}^{-1}$), it has been concluded that the P vacancy is mobile at room temperature (RT).^{29,30} Recent DLTS studies by Massarani *et al.* have shown that this defect level in fact consists of two different hole traps, both associated with the P sublattice.³¹ This study suggests that the fast hole trap $H4_F$, which anneals out below 400 K, could either be a P vacancy or a Frenkel pair ($V_{\text{P}}\text{-P}_i$) and that the slow hole trap $H4_S$ could be the $V_{\text{P}}\text{-Zn}$ pair. The slow trap does not anneal out even after several hours of annealing in 420 K, which is in agreement with our results. However, the introduction rate obtained by Massarani *et al.* for the slow trap $H4_S$ ($\sim 10^{-4} \text{ cm}^{-1}$ at 1 MeV e^- energy) may still be too high for the direct formation of $V_{\text{P}}\text{-Zn}$ during irradiation and thus its formation could require P vacancy migration at RT. When comparing the $H4$ (and $H4_S/H4_F$) level to the ionization level we obtain for the $V_{\text{P}}\text{-Zn}$ pair ($0.2 \pm 0.1 \text{ eV}$) it is not possible to rule out $H4$ as a $V_{\text{P}}\text{-Zn}$ pair.

However, in contradiction with the DLTS results PAS have shown that the P vacancy is stable at RT in electron irradiated InP.^{33,32,4} Similar results have been obtained with PAS for GaInP.³⁴ In agreement with the PAS studies Karsten and Erhart³⁵ and Hausmann and Erhart³⁶ have concluded that the P vacancy becomes mobile at temperatures above 500 K, which is in good agreement with the present study. Hence, we come to the conclusion that the DLTS defect level $H4$ is most likely not the $V_{\text{P}}\text{-Zn}$ pair, rather some other defect in the P sublattice, e.g., a complex of a P interstitial and a Zn dopant.

VI. CONCLUSION

In conclusion, we have used positron annihilation spectroscopy to show that vacancy-type defects are spontane-

ously created in the annealing of heavily Zn-doped InP in the temperature interval 500–700 K. From measured momentum distributions of the annihilating electron-positron pairs we identify the defect as the V_p -Zn pair. We propose a formation model for the defect where native P vacancies migrate and get trapped at Zn atoms. By isothermally annealing the samples, we study the kinetics of the diffusion process. An applied diffusion model yields a migration energy for the P vacancy of 1.8 ± 0.2 eV.

Our data can be used to explain the formation and the

post-growth annealing behavior of V_p -Zn pairs in heavily Zn-doped InP, as well as the presence of native V_p -Zn pairs in Zn doped InP.

ACKNOWLEDGMENTS

The authors acknowledge discussions with Dr. P. Ebert, Professor R. M. Nieminen, Professor M. J. Puska, and Dr. K. Simola. Dr. J. Likonen is acknowledged for performing the SIMS analysis.

-
- ¹S. B. Zhang and J. E. Northrup, *Phys. Rev. Lett.* **67**, 2339 (1991).
²T. Y. Tan, U. Gösele, and S. Yu, *Crit. Rev. Solid State Mater. Sci.* **17**, 47 (1991).
³G. Dlubek, O. Brümmer, F. Plazaola, P. Hautojärvi, and K. Naukarinen, *Appl. Phys. Lett.* **46**, 1136 (1985).
⁴M. Alatalo, H. Kauppinen, K. Saarinen, M. J. Puska, J. Mäkinen, P. Hautojärvi, and R. M. Nieminen, *Phys. Rev. B* **51**, 4176 (1995).
⁵J. Mahony and P. Mascher, *J. Appl. Phys.* **80**, 2712 (1996).
⁶P. Ebert, K. Urban, and M. G. Lagally, *Phys. Rev. Lett.* **72**, 840 (1994).
⁷P. Ebert, M. Heinrich, M. Simon, C. Domke, K. Urban, C. K. Shih, M. B. Webb, and M. G. Lagally, *Phys. Rev. B* **53**, 4580 (1996).
⁸P. Ebert, X. Chen, M. Heinrich, M. Simon, K. Urban, and M. G. Lagally, *Phys. Rev. Lett.* **76**, 2089 (1996).
⁹P. Ebert, M. Heinrich, M. Simon, K. Urban, and M. G. Lagally, *Phys. Rev. B* **51**, 9696 (1995).
¹⁰J. Slotte, K. Saarinen, and P. Ebert (unpublished).
¹¹K. Saarinen, P. Hautojärvi, and C. Corbel, in *Identification of Defects in Semiconductors*, edited by M. Stavola (Academic, New York, 1998).
¹²R. Krause-Rehberg and H. S. Leipner, *Positron Annihilation in Semiconductors* (Springer, Berlin, 1999).
¹³P. Ehrhart, P. Jung, H. Schultz, and H. Ullmaier, *Atomic Defects in Metals* (Springer, Berlin, 1991).
¹⁴S. Dannefaer, P. Mascher, and D. Kerr, *Phys. Rev. Lett.* **56**, 2195 (1986).
¹⁵R. Wurschum, W. Bauer, K. Maier, A. Seeger, and H.-E. Shafer, *J. Phys.: Condens. Matter* **1**, SA33 (1989).
¹⁶J. Gebauer, R. Krause-Rehberg, M. Lausmann, and G. Lippold, *Mater. Sci. Forum* **258-260**, 905 (1997).
¹⁷J. Gebauer, M. Lausmann, F. Redmann, and R. Krause-Rehberg, *Physica B* **274**, 705 (1999).
¹⁸K. Saarinen, P. Hautojärvi, P. Lanki, and C. Corbel, *Phys. Rev. B* **44**, 10 585 (1991).
¹⁹In Ref. 4, where the local density approximation (LDA) scheme has been used in the theoretical calculations, it is in fact suggested that two Zn atoms surround the P vacancy. However, calculations within the generalized gradient approximation (GGA) scheme [M. Alatalo *et al.*, *Phys. Rev. B* **54**, 2397 (1996)], which better takes into account the electron-positron correlation, show that one Zn atom is enough to reproduce the experimental momentum distributions.
²⁰M. Alatalo, R. M. Nieminen, M. J. Puska, A. P. Seitsonen, and R. Virkkunen, *Phys. Rev. B* **47**, 6381 (1993).
²¹H. Xu, *Phys. Rev. B* **42**, 11 295 (1990).
²²W. Walukiewicz, *Phys. Rev. B* **50**, 5221 (1994).
²³G. T. Barkema, P. Biswas, and H. van Beijeren, *Phys. Rev. Lett.* **87**, 170601 (2001).
²⁴H. B. Rosenstock, *J. Math. Phys.* **11**, 487 (1970).
²⁵G. J. van Gorp, T. van Dongen, G. M. Fontijn, J. M. Jacobs, and D. L. A. Tjaden, *J. Appl. Phys.* **65**, 553 (1989).
²⁶G. J. van Gorp, P. R. Boudewijn, M. N. C. Kempeners, and D. L. A. Tjaden, *J. Appl. Phys.* **61**, 1846 (1987).
²⁷*Data in Science and Technology: Semiconductors, Group IV Elements and III-V Compounds*, edited by O. Madelung (Springer-Verlag, Berlin, 1991).
²⁸A. P. Seitsonen, R. Virkkunen, M. J. Puska, and R. M. Nieminen, *Phys. Rev. B* **49**, 5253 (1994).
²⁹A. Sibille and J. Suski, *J. Appl. Phys.* **60**, 595 (1986).
³⁰T. Bretagnon, G. Bastide, M. Rouzeyre, C. Delerue, and M. Lannoo, *Phys. Rev. B* **42**, 11 042 (1990).
³¹B. Massarani, F. G. Awad, M. Kaaka, and R. Darwish, *Phys. Rev. B* **58**, 15 614 (1998).
³²M. Törnqvist, C. Corbel, L. Liszky, K. Saarinen, and P. Hautojärvi, *Mater. Sci. Eng., B* **28**, 126 (1994).
³³M. Törnqvist, J. Nissilä, F. Kiessling, C. Corbel, K. Saarinen, A. P. Seitsonen, and P. Hautojärvi, *Mater. Sci. Forum* **143-147**, 347 (1994).
³⁴J. Dekker, J. Oila, K. Saarinen, A. Tukiainen, W. Li, and M. Pessa, *J. Appl. Phys.* **92**, 5942 (2002).
³⁵K. Karsten and P. Ehrhart, *Phys. Rev. B* **51**, 10 508 (1995).
³⁶H. Hausmann and P. Ehrhart, *Phys. Rev. B* **51**, 17 542 (1995).